Photoluminescence dynamics in GaAs/AlAs quantum wells modulated by one-dimensional standing surface acoustic waves

Tetsuomi Sogawa,[1,a)] Haruki Sanada,[1] Hideki Gotoh,[1] Hiroshi Yamaguchi,[1] Sen Miyashita,[2] and Paulo V. Santos[3]
[1]*NTT Basic Research Laboratories, NTT Corporation, 3-1 Morinosato-Wakamiya, Atsugi, Kanagawa 243-0198, Japan*
[2]*NTT Advanced Technology Corporation, 3-1 Morinosato-Wakamiya, Atsugi, Kanagawa 243-0198, Japan*
[3]*Paul Drude Institute, Hausvogteiplatz 5-7, 10117 Berlin, Germany*

(Received 20 December 2008; accepted 13 March 2009; published online 1 April 2009)

The effects of standing surface acoustic waves (SAWs) on carrier dynamics in GaAs/AlAs quantum wells are investigated by spatially and time-resolved photoluminescence (PL) spectroscopy. We found that the PL spectra vary considerably depending on the position and the phase of the standing SAW field. The PL spectra are characterized by oscillations in the PL intensity and emission energy due to the motion of free carriers and excitons driven by the piezoelectric fields as well as by the strain-induced band-gap gradient. It is also demonstrated that the positions of the nodes and antinodes of the standing SAW are precisely controlled. © *2009 American Institute of Physics*. [DOI: 10.1063/1.3114382]

There has been considerable interest in the use of surface acoustic waves (SAWs) to modulate the in-plane electronic properties of quantum well (QW) structures.[1–8] In piezoelectric materials such as GaAs, SAWs can be easily generated by applying a radio frequency (rf) voltage to interdigital transducers (IDTs) deposited on the sample surface. It has been demonstrated that the SAW-induced lateral piezoelectric field separates electrons and holes and thus quenches the photoluminescence (PL) intensity.[2,8] The electrons and holes are trapped at the maxima and minima of the SAW piezoelectric potential (Φ_{SAW}), where they are transported with the SAW velocity of approximately 3000 m/s in GaAs. The transported carriers can be forced to recombine at a particular position if a metal film is deposited on the surface to short-circuit Φ_{SAW}. Interestingly, unique optical properties such as polarization anisotropy of the PL due to strain-induced band mixing[5,8] as well as spin manipulation capability[9–11] have also been reported. In addition, dimensionality oscillation due to the standing SAW fields has been demonstrated.[12] These unique optical and electrical properties in dynamically modulated structures have been attracting increasing attention from the viewpoint of fundamental physics as well as device applications. In this study, we investigate the mechanism for the PL modulation of GaAs/AlAs QWs in the space and time domains by a one-dimensional standing SAW field, formed by the interference of two counterpropagating SAW beams. Time- and spatially resolved PL spectra clearly demonstrate that the carriers are driven by the oscillating piezoelectric and strain fields. It is also shown that the positions of the nodes and antinodes of the standing SAW field are electrically controlled.

In the experiment, we have used high-quality GaAs/AlAs QWs with various well thicknesses (L_z=6.3, 7.1, 8.3, 9.9, 12.2, 15.2, 19.8, and 83 nm), which were grown by molecular-beam epitaxy on GaAs (001) substrate. The QWs are located between 100 and 400 nm from the surface. Each QW is separated from the others by AlAs (2.0 nm)/GaAs (2.0 nm) superlattice barrier layers with a total thickness of 26 nm. Two IDTs, separated by 500 μm, were deposited on the surface to generate SAWs propagating along the [110] and [$\bar{1}\bar{1}$0] directions. As the SAW frequency is 820 MHz, the SAW period (T_{SAW}) and the SAW wavelength (λ_{SAW}) correspond to 1.2 ns and approximately 3.6 μm, respectively. Mode-locked Ti-sapphire laser pulses (1.5 ps, 82 MHz, and 720 nm), which are synchronized with the SAWs, were used to generate carriers with a repetition period equal to $10T_{SAW}$. Low-temperature (4 K) spatial-resolved PL spectra were measured using a micro-PL setup with a spatial resolution of approximately 1 μm. The PL was spectrally analyzed by a spectrometer connected to a synchronously (82 MHz) scanning streak camera with a time resolution of 10 ps. We used SAWs with a linear power density P_l of approximately 100 W/m per beam, where P_l is defined as the acoustic power flux per unit length along the cross section of the SAW beam.

The acoustic field of Rayleigh SAW waves propagating along the x and $-x$ directions can be approximately expressed as $\sin(kx-\omega t-\theta_1)$ and $\sin(-kx-\omega t-\theta_2)$, respectively, where k is the wave number, ω is the angular frequency, and $\theta_1(\theta_2)$ is the relative phase between the laser pulse and the SAW field propagating in the x ($-x$) direction. The interference of these counterpropagating SAWs forms a standing wave, described as

$$-2\cos[kx-(\theta_1-\theta_2)/2]\sin[\omega t+(\theta_1+\theta_2)/2]. \quad (1)$$

This formula indicates that the term $(\theta_1-\theta_2)/2$ determines the spatial shift in the nodes and antinodes, while $(\theta_1+\theta_2)/2$ alters the relative phase between the laser pulse and the SAW field. An inset of Fig. 1 schematically shows the changes in the band structure modulated by the standing SAW under the assumption that the interference cancels the modulation at $t=0[\theta_1=\theta_2=0]$. The dashed lines display the modulation of the electronic energy $(-q\Phi_{SAW})$ for the conduction band (CB) and heavy-hole (HH) band while the solid lines represent the strain-induced energy shifts in the CB and HH under a standing SAW along the [110] direction. The type of band-gap modulation by the SAW strain depends on

a)Electronic mail: sogawa.tetsuomi@lab.ntt.co.jp.

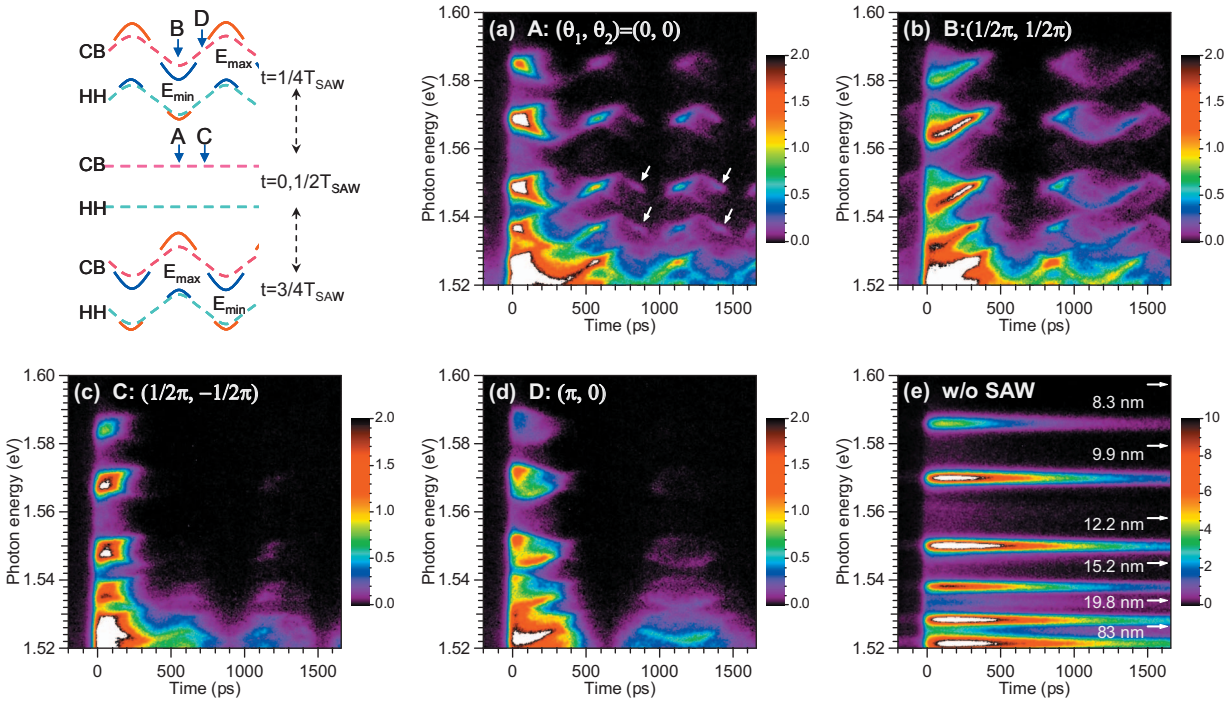

FIG. 1. (Color) An inset illustration schematically shows changes in the band structure modulated by a standing SAW. [(a)–(d)] Time-resolved PL spectra measured at the same position under the standing SAW with different phases of $(\theta_1, \theta_2)=(0,0)$, $(1/2\pi, 1/2\pi)$, $(1/2\pi, -1/2\pi)$, and $(\pi, 0)$, respectively. (e) Corresponding spectrum in the absence of a SAW.

the depth from the surface relative to λ_{SAW} (Ref. 13) and is of type II for the QWs used in this experiment. E_{max} (E_{min}) denotes the positions, where the band-gap energy is a maximum (minimum) due to the compressive (tensile) SAW strain. At the antinode positions, the band-gap energy oscillates between E_{max} and E_{min} with a period of T_{SAW}, and a flatband condition appears every $T_{SAW}/2$.

Figures 1(a)–1(d) display time-resolved PL spectra measured at a fixed laser spot position under the standing SAW field with different phases (θ_1, θ_2) given by $A=(0,0)$, $B=(1/2\pi, 1/2\pi)$, $C=(1/2\pi, -1/2\pi)$, and $D=(\pi, 0)$, respectively, where $t=0$ corresponds to the laser excitation. For comparison, the corresponding spectrum in the absence of a SAW is shown in Fig. 1(e), where white arrows denote the band-to-band transition edges, which are determined by the measurement of PL excitation spectra (not shown here). The phases were precisely changed by shifting the relative phases between the rf trigger signal for the laser driver and the rf voltage signals applied to the two IDTs. The standing SAW drastically alters the PL dynamics from the monotonic decrease in the PL intensity, which is observed in the absence of a SAW [Fig. 1(e)], into a spectrum characterized by oscillations in the PL intensity and emission energy. The change in emission energy could be caused by the quantum confined stark effect (QCSE) induced by the SAW-induced vertical piezoelectric field at the antinodes.[8] However, the energy shifts by the QCSE should sensitively depend on L_z, in contrast to Fig. 1, which clearly does not exhibit an L_z dependence. Thus, the observed energy shifts are attributed to the band-gap modulation induced by the SAW strain. Figures 1(a)–1(d) show that the PL dynamics vary sensitively depending on the combination of phases (θ_1, θ_2), which shifts the SAW field in the space and time domains, as described by Eq. (1). The capital letters A–D, denoted in the inset of Fig. 1, indicate the laser excitation positions and phases used to record the spectra in Figs. 1(a)–1(d), respectively.

Condition A $[(\theta_1, \theta_2)=(0,0)]$ corresponds to the pulse excitation at the antinode, when the band structure is flat. Figure 1(a) shows that the PL intensity becomes prominent every $T_{SAW}/2$. Note that the PL emission energies coincide with the ones measured in the absence of a SAW, thus demonstrating that the emissions occur when the band-gap modulation disappears. For condition B $[(\theta_1, \theta_2)=(1/2\pi, 1/2\pi)]$, the laser spot also impinges on an antinode. Due to the delay of the laser pulse by $T_{SAW}/4=300$ ps relative to A, however, the excitation takes place when the band gap is minimum. As a result, the emission energies in Fig. 1(b) start from the shrunk band-gap energies and progressively increases until the flatband condition is achieved at $t=300$ ps. Then, PL disappears after $t=400$ ps and appears again around $t=900$ ps.

Figures 2(a)–2(c) show normalized PL time traces under conditions A–C, respectively, for the five QWs (L_z=8.3, 9.9, 12.2, 15.2, and 19.8 nm), where the PL spectra were selectively integrated at the flatband photon energies of 1.527, 1.537, 1.549, 1.569, and 1.585 eV. The positions of the PL peaks in Fig. 2(a) clearly demonstrate that the flatband condition is reached around $t=0$, 550, and 1150 ps. In Fig. 2(b), the PL peaks are delayed by approximately 300 ps $(1/4T_{SAW})$ with respect to those in Fig. 2(a). In Fig. 1(a), weak emissions are observed at $t=800$ and 1400 ps, as indicated by white arrows. These signals are artifact induced by the backward sweep of the synchronously (82 MHz) scanning streak camera because the camera superimposes the PL signal recorded during the backward sweep at time $t+6$ ns on the PL signal detected at time t.

Conditions C [Fig. 1(c)] and D [Fig. 1(d)] correspond to the excitation at the node when the modulation is absent and maximum, respectively. At the nodes, the PL energy should be constant due to the absence of band-gap modulation,

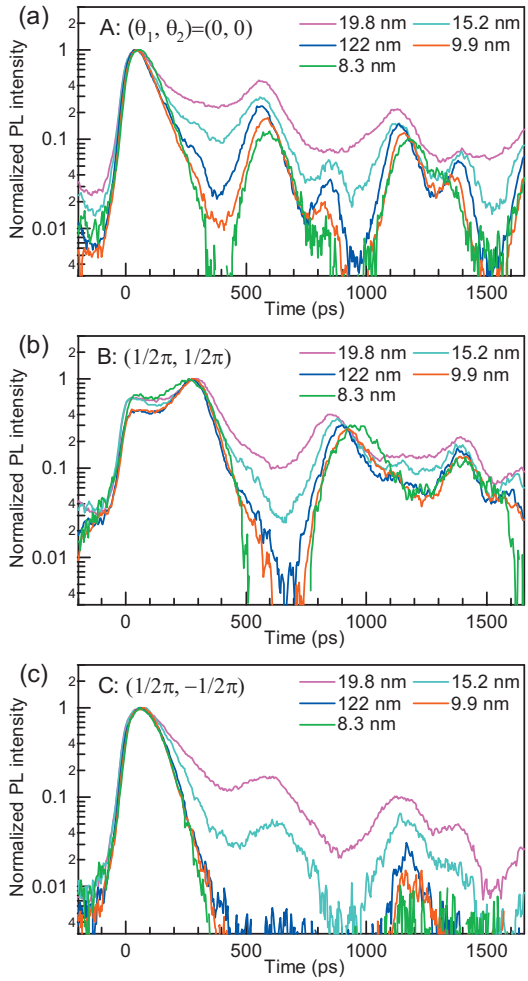

FIG. 2. (Color) [(a)–(c)] Normalized time traces for the 8.3, 9.9, 12.2, 15.2, and 19.8 nm QWs under a standing SAW with $(\theta_1, \theta_2)=(0,0)$, $(1/2\pi, 1/2\pi)$, and $(1/2\pi, -1/2\pi)$, respectively. The PL intensity was selectively integrated at the photon energies of 1.527, 1.537, 1.549, 1.569, and 1.585 eV.

while the lateral field is continuously varying. In Fig. 1(c), PL emissions with relatively narrow linewidth occur just after the excitation. The subsequent emissions, which appear around $t=600$ ps ($T_{SAW}/2$) and 1.2 ns (T_{SAW}), seem to be very weak except for the thick QWs ($L_z \geq 15.2$ nm) [cf. Fig. 2(c)]. It is because the strong lateral piezoelectric field ionizes the excitons. Even if some part of the excitons is not ionized, they do not stay at the node position but move toward E_{min} driven by the effective field due to the band-gap gradient.[12] Note that Fig. 1(d) exhibits PL energy splitting. Just after the excitation ($t=0-100$ ps), the higher-energy emissions are larger than the lower-energy ones. Then ($t>100$ ps), the higher-energy ones decrease, while lower-energy ones begin to increase. The PL splitting is attributed to the fact that the emissions from the nodes, which should coincide with the flatband energies, are suppressed due to the strong piezoelectric or effective fields and that the emissions originating from the vicinity of E_{max} and E_{min} areas are simultaneously detected because of the insufficiently small spatial resolution (with a full width at half maximum of approximately 1 μm). A possible reason for the appearance of the higher-energy emissions just after the excitation ($t=0-100$ ps) is that the excitation position is slightly shifted from the node toward E_{max}.

For the discussion on the exciton migration and diffusion, it should be considered that the mobility and diffusivity of excitons depend on L_z.[12,14] Figure 1(d) shows that relative intensities for the lower-energy emissions become stronger as L_z increases, indicating that the exciton migration into E_{min} is enhanced in thick QWs. The poor contrast of the PL intensity modulation in thick QWs, as observed in Figs. 2(a)–2(c), is also due to the long exciton diffusion length with respect to the separation between E_{max} and E_{min}, i.e., $\lambda_{SAW}/2=1.8$ μm.

We have investigated the effects of SAWs on the PL dynamics of GaAs/AlAs QWs. Spatially and time-resolved PL measurements reveal that the PL spectra reflect the carrier dynamics driven by the oscillating piezoelectric and strain fields. It has been demonstrated that node and antinode positions of the standing SAW can be precisely tuned. We found that PL emission mainly takes place at the antinode positions due to the exciton migration toward the local minima of the band-gap modulation, while at the nodes carriers do not stay stable due to the temporally varying lateral fields.

We gratefully acknowledge H. Kamada, T. Tawara, Y. Hirayama, and K. Ploog for fruitful discussion and comments. This work was partly supported by Grant-in-Aid for Scientific Research from the Japan Society for the Promotion of Science (Grant No. 19310067).

[1] J. M. Shilton, V. I. Talyanskii, M. Pepper, D. A. Ritchie, J. E. F. Frost, C. J. B. Ford, C. G. Smith, and G. A. C. Jones, J. Phys.: Condens. Matter **8**, L531 (1996).
[2] C. Rocke, S. Zimmermann, A. Wixforth, J. P. Kotthaus, G. Böhm, and G. Weimann, Phys. Rev. Lett. **78**, 4099 (1997).
[3] P. V. Santos, M. Ramsteiner, and F. Jungnickel, Appl. Phys. Lett. **72**, 2099 (1998).
[4] P. V. Santos, Appl. Phys. Lett. **74**, 4002 (1999).
[5] T. Sogawa, P. V. Santos, S. K. Zhang, S. Eshlaghi, A. D. Wieck, and K. H. Ploog, Phys. Rev. B **63**, 121307(R) (2001).
[6] F. Alsina, P. V. Santos, R. Hey, A. García-Cristóbal and A. Cantarero, Phys. Rev. B **64**, 041304(R) (2001).
[7] F. Alsina, J. A. H. Stotz, R. Hey, and P. V. Santos, Solid State Commun. **129**, 453 (2004).
[8] P. V. Santos, F. Alsina, J. A. H. Stotz, R. Hey, S. Eshlaghi, and A. D. Wieck, Phys. Rev. B **69**, 155318 (2004).
[9] T. Sogawa, P. V. Santos, S. K. Zhang, S. Eshlaghi, A. D. Wieck, and K. H. Ploog, Phys. Rev. Lett. **87**, 276601 (2001).
[10] J. A. H. Stotz, R. Hey, P. V. Santos, and K. H. Ploog, Nature Mater. **4**, 585 (2005).
[11] O. D. D. Couto, Jr., F. Iikawa, J. Rudolph, R. Hey, and P. V. Santos, Phys. Rev. Lett. **98**, 036603 (2007).
[12] T. Sogawa, H. Gotoh, Y. Hirayama, P. V. Santos, and K. H. Ploog, Appl. Phys. Lett. **91**, 141917 (2007).
[13] J. Rudolph, R. Hey, and P. V. Santos, Phys. Rev. Lett. **99**, 047602 (2007).
[14] T. Sogawa, H. Sanada, H. Gotoh, H. Yamaguchi, S. Miyashita, and P. V. Santos, Jpn. J. Appl. Phys., Part 2 **46**, L758 (2007).